NIH Public Access
Author Manuscript
Exp Cell Res. Author manuscript; available in PMC 2010 April 15.

Published in final edited form as:
Exp Cell Res. 2009 April 15; 315(7): 1234–1246. doi:10.1016/j.yexcr.2009.01.021.

Live-cell imaging demonstrates extracellular matrix degradation in association with active cathepsin B in caveolae of endothelial cells during tube formation

Dora Cavallo-Medved[1,2,*], **Deborah Rudy**[1], **Galia Blum**[3], **Matthew Bogyo**[3,4], **Dejan Caglic**[5], and **Bonnie F. Sloane**[1,2]

1 *Department of Pharmacology, Wayne State University, School of Medicine, Detroit, Michigan 48201, USA*

2 *Barbara Ann Karmanos Cancer Institute, Wayne State University, School of Medicine, Detroit, Michigan 48201, USA*

3 *Department of Pathology, Stanford University, School of Medicine, Stanford, California 94305, USA*

4 *Department of Microbiology and Immunology, Stanford University, School of Medicine, Stanford, California 94305, USA*

5 *Department of Biochemistry, and Molecular and Structural Biology, Jozef Stefan Institute, Jamova 39, 1000 Ljubljana, Slovenia*

Abstract

Localization of proteases to the surface of endothelial cells and remodeling of the extracellular matrix (ECM) are essential to endothelial cell tube formation and angiogenesis. Here, we partially localized active cathepsin B and its cell surface binding partners, S100A/p11 (p11) of the annexin II heterotetramer (AIIt), to caveolae of human umbilical vein endothelial cells (HUVEC). Via a live-cell proteolysis assay, we observed that degradation products of quenched-fluorescent (DQ)-proteins (i.e. gelatin and collagen IV) colocalized intracellularly with caveolin-1 (cav-1) of HUVEC grown in either monolayer cultures or *in vitro* tube formation assays. Activity-based probes that bind covalently to active cysteine cathepsins and degradation products of DQ-collagen IV partially localized to intracellular vesicles that contained cav-1 and active cysteine cathepsins. Biochemical analyses revealed that the distribution of active cathepsin B in caveolar fractions increased during *in vitro* tube formation. Pro-uPA, uPAR, MMP-2 and MMP-14, which have been linked with cathepsin B to ECM degradation pathways, were also found to increase in caveolar fractions during *in vitro* tube formation. Our findings are the first to demonstrate through live-cell imaging ECM degradation in association with active cathepsin B in caveolae of endothelial cells during tube formation.

Keywords

Endothelial cells; caveolae; cathepsin B; proteases; ECM degradation; angiogenesis; functional imaging

*Correspondence to: Dora Cavallo-Medved, Dept. of Pharmacology, Wayne State University, 540 East Canfield, Detroit, MI 48201, Tel.: 313-577-4451 (office) and 313-577-1112 (laboratory); Fax: 313-577-6739; E-mail: E-mail: dcavallo@med.wayne.edu.

Publisher's Disclaimer: This is a PDF file of an unedited manuscript that has been accepted for publication. As a service to our customers we are providing this early version of the manuscript. The manuscript will undergo copyediting, typesetting, and review of the resulting proof before it is published in its final citable form. Please note that during the production process errors may be discovered which could affect the content, and all legal disclaimers that apply to the journal pertain.

NIH-PA Author Manuscript
NIH-PA Author Manuscript
NIH-PA Author Manuscript

NIH-PA Author Manuscript

NIH-PA Author Manuscript

NIH-PA Author Manuscript

Introduction

Angiogenesis, the formation of new blood vessels from the pre-existing vasculature, is a process in which stimulated endothelial cells remodel extracellular matrix (ECM), migrate through the ECM, proliferate, differentiate and eventually form endothelial tubules capable of blood transport [1]. Proteases of at least three classes (serine, cysteine, and metallo-) [including matrix metalloproteinases (MMPs), members of the urokinase plasmin(ogen) system and cysteine cathepsins] play crucial roles in angiogenesis (for review see [2]). Proteases participate in the angiogenic process by generating both pro- and anti-angiogenic factors from ECM proteins [3–5] and by processing growth factors and receptors, including integrins [6,7]. For example, cleavage of type IV collagen by endothelial cell MMPs results in the exposure of cryptic αvβ3-integrin binding sites, thus promoting angiogenesis [7]. Urokinase plasminogen activator (uPA) converts plasminogen to plasmin which can be further processed to generate angiostatin, an anti-angiogenic compound [8]. Cathepsin B, a lysosomal cysteine protease, regulates the “angiogenic switch” [9] by initiating proteolytic cascades involved in ECM degradation that promote angiogenesis [10], or conversely, by cleaving collagen XVIII and generating endostatin, an anti-angiogenic factor [11]. Overall, the balance of protease activity and the interaction of proteases with the ECM contribute to regulation of the angiogenic process.

ECM remodeling and degradation by tumor cells are facilitated by the translocation of proteases to cell surfaces and their secretion into the extracellular milieu [12–15]. Many proteases implicated in ECM remodeling and degradation are also associated with caveolae [12], a lipid-rich region of the plasma membrane involved in endocytosis, cholesterol transport and cell signaling events (for reviews, see [16,17]). These proteases include uPA and its receptor uPAR, cathepsin B and its cell surface binding protein S100A10/p11 (p11) [the light chain of the annexin II heterotetramer (AIIt)], MMP-2 and MMP-14 [12]. In colorectal carcinoma cells, downregulation of caveolin-1 (cav-1), the main structural protein of caveolae, decreases distribution of cathepsin B and uPA to caveolae and ECM degradation by these cells [18]. The association of proteases with caveolae of endothelial cells is intriguing since caveolae are involved in angiogenesis (for review, see [19]). During endothelial cell migration, cav-1 localizes to the rear of migrating cells [20–22]. Moreover, downregulation of cav-1 impedes endothelial cell polarization and directional movement [20]. Indeed, knockdown of cav-1 suppresses tube formation by endothelial cells and also reduces vessel formation in the chicken chorioallantoic membrane assay [23]. Thus, we hypothesize that compartmentalization of proteases to caveolae in endothelial cells modulates cell migration, proteolysis of ECM proteins and tube formation.

In the present study, we identified active cathepsin B as well as its cell surface-binding partner, S100A10/p11 (p11), in caveolae of human umbilical vein endothelial cells (HUVEC): an association that is augmented during *in vitro* endothelial tube cell formation. Using a live-cell proteolysis assay in combination with *in vitro* tube formation assays and cysteine cathepsin activity-based probes, we observed extracellular degradation of ECM proteins (i.e., type IV collagen) by migrating HUVEC and intracellular colocalization of ECM degradation products with cav-1 in vesicles containing active cysteine cathepsins. These data suggest an association of active cathepsin B with caveolae and degradation and remodeling of the ECM during endothelial cell migration and tube formation.

Materials and Methods

Materials

M199 medium, heparin, N-Octyl β-D-glucopyranoside, 2-[N-morpholino]ethanesulfonic acid (MES), methyl-β-cyclodextrin (MβCD), and all other chemicals unless otherwise stated were

NIH-PA Author Manuscript

NIH-PA Author Manuscript

NIH-PA Author Manuscript

from Sigma (St. Louis, MO); fetal bovine serum (FBS), Lipofectin reagent, dye-quenched fluorescent (DQ)-gelatin and DQ-collagen IV were from Invitrogen (Carlsbad, CA); bovine endothelial cell growth factor (bECGF) was from Roche Applied Science (Indianapolis, IN); polyclonal anti-caveolin (610059), monoclonal anti-annexin II (mAb 5) and monoclonal anti-p11 (mAb 148) antibodies were purchased from BD Biosciences (Bedford, MA); polyclonal anti-cathepsin B [24] antibodies were produced, affinity-purified and characterized in our laboratory; polyclonal anti-β1 integrin antibodies were a kind gift from Dr. Kenneth Yamada (National Institutes of Health/National Institute of Dental and Craniofacial Research, Bethesda, MD); polyclonal anti-uPA (ab20046) and polyclonal anti-uPAR (ab27423) antibodies were from Abcam (Cambridge, MA); polyclonal anti-MMP-14 (AB815) antibodies were from Chemicon (Temecula, CA); horseradish peroxidase-labeled goat anti-rabbit and goat anti-mouse IgG were from Pierce (Rockford, IL); purified MMP-2 and MMP-9 enzymes were a kind gift from Dr. Rafael Fridman (Wayne State University, Detroit, MI); cysteine cathepsin activity-based probes, GB-111-FL and GB-123, were recently described in references [25] and [26], respectively; Cultrex was from Trevigen (Gaithersberg, MD); acrylamide and nitrocellulose membranes were from BioRad (Hercules, CA); protein markers and chemiluminescent western blotting detection kits were from Amersham Pharmacia Biotech (Piscataway, NJ); benzyloxycarbonyl-L-arginyl-L-arginine-4-methyl-7-coumarylamide (Z-Arg-Arg-NHMec) was from Bachem (Torrance, CA); and Amicon Ultra-4 10 K centrifugal filters were from Millipore (Bedford, CA).

Cell Culture

HUVEC from the American Type Culture Collection (ATCC) (Rockville, MD) were grown on 1.5% (w/v) gelatin-coated tissue culture lab-ware in endothelial cell M199 media supplemented with 40 μg/ml bECGF, 100 μg/ml heparin, antibiotics (penicillin/streptomycin) and 10% (v/v) FBS (as recommended by the ATCC) in 5% CO_2/humidified atmosphere at 37° C unless otherwise stated.

Transient transfection of HUVEC with cav-1-mRFP expression vector (a kind gift from Drs. Radu V. Stan and Steve F. Dowdy, University of California at San Diego, San Diego, CA) was performed using Lipofectin reagent according to the manufacturer's instructions.

In vitro Tube Formation Assay

In vitro tube formation assays were performed in 35 mm tissue culture dishes coated with 200 μl of Cultrex [i.e., reconstituted basement membrane (rBM)] that was allowed to gel at 37 °C for 10 min. Thereafter, 2×10^5 cells were seeded onto the Cultrex in M199 media containing 2% (v/v) FBS and incubated at 37 °C for 16–18 h to allow formation of tubular structures [27,28].

Preparation of caveolae-enriched fractions

Caveolae-enriched fractions were isolated by both non-detergent and detergent based methods. The non-detergent method was performed as previously described [18,29]. Briefly, cells from four 100 mm dishes were washed twice with PBS at 4°C and lysed in 2 ml 500 mM sodium carbonate buffer, pH 11.0. Cell lysates were homogenized on ice by 10 strokes in a loose-fitting Dounce homogenizer and then sonicated on ice in a 50 W ultrasonicator three times for 20 sec each. Cell homogenates were adjusted to 45% (w/v) sucrose by mixing them with 2 ml of 90% (w/v) sucrose prepared in MES-buffered saline (25 mM MES, pH 6.5, 0.15 m NaCl) and then placed on the bottom of a 12 ml ultracentrifuge tube. The homogenate was then overlaid with a 5–-35% sucrose gradient comprised of 4 ml of 35% (w/v) sucrose (in MES-buffered saline containing 250 mM sodium carbonate) and 4 ml of 5% (w/v) sucrose (in MES-buffered saline containing 250 mM sodium carbonate). Gradients were subjected to ultracentrifugation at 185,000 g in a SW41 rotor (Beckman Instruments) for 18–20 h at 4 °C. One ml fractions were

NIH-PA Author Manuscript

NIH-PA Author Manuscript

NIH-PA Author Manuscript

collected from the top of the gradient and equal volume aliquots were analyzed by SDS-PAGE and immunoblotting. Where indicated, cells were treated overnight with 1 μM GB111-FL, a quenched activity-based probe for cysteine cathepsins [25], prior to caveolae isolation. SDS-PAGE gels were imaged on a Typhoon Imaging Scanner (Amersham Biosciences, Pittsburgh, PA) to detect bound probe.

Caveolae-enriched fractions could not be isolated from HUVEC grown on rBM for *in vitro* tube-formation assays using the non-detergent based method described above because the amount of rBM (131.2 mg in 8 ml) required for sufficient cells, i.e., four 100 mm dishes, prevented proper preparation of sucrose gradients. Therefore, we employed a successive detergent based method that separates Triton X-100-soluble from -insoluble membrane components [30]. Cells were incubated in lysis buffer containing 1% Triton X-100 in the absence of octylglucoside for 30 min on ice, collected and centrifuged at 14,000 × g for 15 min at 4 °C. The supernatant, hereafter termed the Triton-soluble fraction, was recovered. The insoluble pellet was resuspended in an equal volume of lysis buffer containing both 1% Triton X-100 and 60 mM octylglucoside, incubated on ice for 30 min, passed 10 times through a syringe with a 20-gauge needle and centrifuged for 10 min at 14,000 × g at 4 °C. The supernatant, hereafter termed the Triton-insoluble fraction, was recovered and the final volume adjusted to that of the Triton-soluble fraction. Caveolae were enriched in the Triton-insoluble fraction as was verified by treating cells with 10 mM MβCD, a cholesterol sequestering drug that disrupts caveolae, at 37 °C for 1 h prior to successive detergent extraction of membranes.

Preparation of Conditioned Media

Equal numbers of cells were serum-starved overnight, media were collected, centrifuged at 800 × g to remove whole cells, re-centrifuged at 2,000 × g to remove cell debris, and concentrated to equal final volumes.

SDS-PAGE and Immunoblot Analysis

Samples were equally loaded and separated by SDS-PAGE (10%, 12% or 15% acrylamide) and transferred onto nitrocellulose membranes under either reducing or non-reducing conditions. Immunoblotting was performed with primary antibodies against cathepsin B (1:4000), caveolin (1:5000), annexin II (1:5000), p11 (1:5000), uPA (5 μg/ml), uPAR (5 μg/ml), β1-integrin (1:3000) and MMP-14 (1:1000) and secondary antibodies conjugated with horseradish peroxidase (1:10,000) in Tris-buffered saline wash buffer (20 mM Tris, pH 7.5, 0.5 M NaCl) containing 0.5% Tween 20 and 5% (w/v) non-fat dry milk. After washing, bound antibodies were detected by enhanced chemiluminescence according to the manufacturer's instructions.

Gelatin Zymography

Subcellular fractions and conditioned media samples were equally loaded and applied without heating or reduction to a 10% SDS-polyacrylamide gel containing 1 mg/ml of gelatin [31]. After electrophoresis, the gel was washed twice for 15 min each time with 2.5% Triton X-100, followed by a 20 min wash with distilled water, and incubated overnight at 37 °C in 50 mM Tris buffer, pH 7.8, containing 5 mM $CaCl_2$ and 0.05% Brij35. The gel was stained with a solution of 0.5% Coomassie brilliant blue R-250 in 50% methanol and 10% acetic acid and then de-stained in a 50% methanol and 10% acetic acid solution. Clear bands represent areas of proteolytic activity. Purified MMP-2 and MMP-9 were loaded separately as positive controls.

NIH-PA Author Manuscript

NIH-PA Author Manuscript

NIH-PA Author Manuscript

Cathepsin B Activity Assay

Cathepsin B activity was measured in subcellular fractions and conditioned media as previously described [32]. Briefly, to measure intracellular cathepsin B activity 50 μl of sample was incubated with 300 μl of activator buffer (5 mM EDTA, 10 mM DTT, pH 5.2) for 15 min at 37 °C. In a 96 well flat-bottom black microtiter plate, 100 μl of cell lysate/activator buffer mixture was added to 200 μl of assay buffer [Hank's balanced-salt solution lacking sodium bicarbonate and phenol red and containing 0.6 mM $CaCl_2$, 0.6 mM $MgCl_2$ and 25 mM piperazin-N-N′-bis[2-ethanesμlfonic acid] (disodium salt), pH 7.3] containing 150 μM Z-Arg-Arg-NHMec substrate. The enzymatic assay was carried out at pH 6.0. Fluorescence was measured in triplicate at one-minute intervals for 30 minutes using a Tecan SpectraFluor Plus plate-reader at an excitation of 360 nm and an emission of 465 nm. To measure latent or procathepsin B activity in media samples, autoactivation of procathepsin B was accelerated in the presence of dextran sulfate [33]. Briefly, 50 μl of conditioned media was mixed with 300 μl of citrate buffer (20 mM citrate buffer, pH 4.6, 10 mM DTT and 25 μg/ml dextran sulfate) and incubated for 45 min at 37 °C. Then 100 μl of media-citrate buffer solution was mixed in a 96 well flat-bottom black microtiter plate with 200 μl of 150 μM Z-Arg-Arg-NHMec substrate prepared in 200 mM sodium phosphate buffer, pH 6.8. Fluorescence was read in triplicate at one-minute intervals over a 30 min period at an excitation of 360 nm and an emission of 465 nm. Cathepsin B activity was recorded as pmoles/min/cell number. Cells were counted using a hemocytometer prior to setting up overnight experiments. Statistical significance was determined by a two-tailed t-test with assumed equal variance. In the figures, * represents a p value less than 0.05 and ** represents a p value less than 0.01.

Immunocytochemistry

Cells were grown on coverslips for 16–24 hours, permeabilized with saponin, fixed with cold methanol for 5 min and then blocked for 45 minutes by incubating with PBS containing 2 mg/ml BSA. Cells were then washed with PBS and incubated with primary antibody (rabbit anti-human caveolin or preimmune rabbit IgG) for 2 hours at room temperature according to our published procedures [34]. After washing with PBS, the cells were incubated for 1 hour with Texas red-conjugated affinity-purified donkey anti-rabbit IgG containing 5% normal donkey serum (Jackson ImmunoResearch). Cells were then washed, mounted upside-down with Slow Fade anti-fade reagent (Invitrogen Life Technologies) on glass slides and observed with a Zeiss 510 LSM confocal microscope.

Live Cell Proteolysis Assay

Proteolysis by live cells was assessed as previously described [35,36]. Briefly, glass coverslips were coated with either 50 μl of 1.5% (w/v) gelatin containing 25 μg/ml DQ-gelatin and incubated on ice for 15 min to solidify or 50 μl of 16.4 mg/ml Cultrex containing 25 μg/ml DQ-collagen IV and incubated for 10 min at 37 °C to solidify. Subsequent steps were carried out at 37 °C. Cells (2.5×10^4) were seeded onto coated coverslips and incubated for 60 min. Medium containing 2% FBS was added to the cells and incubated for 16–18 h. Proteolysis of DQ-gelatin and DQ-collagen IV (green fluorescence) was observed in live cells with a Zeiss LSM 510 META NLO microscope with 10x and 40x water immersion objectives. Time series analyses of DQ-collagen IV degradation were performed with a Zeiss LSM 510 META NLO microscope equipped with a controlled environmental chamber that maintains a 5% CO_2/humidified atmosphere at 37 °C. Where indicated, assays were conducted in the presence of 1 μM GB-123, a non-quenched cysteine cathepsin activity-based probe, for 16–18 h. Cells were washed 3 times with PBS and incubated in complete growth medium in the absence of the probe immediately prior to imaging.

NIH-PA Author Manuscript

NIH-PA Author Manuscript

NIH-PA Author Manuscript

Results

Gelatin and collagen IV degradation products localize to vesicles containing cav-1 in HUVEC

Remodeling of the ECM is a process critical to the formation of tubular structures by endothelial cells. To analyze this process, we employed a well-established live-cell proteolysis assay [35] and compared HUVEC grown on coverslips coated with gelatin containing DQ-gelatin with HUVEC grown on coverslips coated with rBM containing DQ-collagen IV. Following 16 h of incubation, live cells were imaged by confocal microscopy for degradation products (green fluorescence) of the two DQ-protein substrates. On gelatin, HUVEC grew as a monolayer of individual cells (Figure 1A) and degradation products of DQ-gelatin were observed primarily intracellularly in the perinuclear region (Figure 1B). In comparison, HUVEC grown on rBM were stimulated to migrate and form large multicellular structures often referred to as “cord-like”, “tube-like” or “tubular” structures (Figure 1C), thus mimicking angiogenesis *in vitro*, a process hereafter referred to as tube formation [27,28]. Degradation products of DQ-collagen IV were localized both intracellularly and pericellularly (i.e., on the cell membrane and immediately outside the cell) (Figure 1D).

To assess whether cav-1, the main structural protein for caveolae, is associated with ECM degradation, we first immunostained HUVEC grown in monolayer versus tube-like structures for endogenous cav-1. Under both conditions, endogenous cav-1 (green fluorescence) was localized both within intracellular perinuclear vesicles and along the surface of HUVEC cells (Figure 1E–H). We were unable to determine whether endogenous cav-1 colocalized with degradation products of DQ-substrates as the fixation required for immunostaining interferes with the fluorescence emitted by the DQ-substrate degradation products. Therefore, we performed a live-cell proteolysis assay with cav-1-mRFP transfected HUVEC cells. The images in Figure 2A and B illustrate that cav-1-mRFP (red fluorescence) and DQ-substrate degradation products (green fluorescence) colocalized in a perinuclear punctate pattern, a pattern similar to that observed for the DQ-substrate degradation products in Figure 1, suggesting that ECM degradation in HUVEC grown as a 2D monolayer and as 3D tube-like structures occurs within vesicles containing caveolin-1, or that ECM degradation products are internalized via caveolae.

Cathepsin B and its cell surface binding partner partially co-localize to caveolae of HUVEC

We have previously established that cathepsin B is present in caveolae of human colorectal carcinoma cells [34]. Here, we examined the colocalization of cathepsin B with cav-1 in caveolae of HUVEC. Isolation of caveolae from HUVEC in monolayer culture was performed using a well-established protocol that is based on the insolubility of caveolae to carbonate extraction and their specific buoyant density in equilibrium sucrose gradients [29]. Cav-1, a marker protein for caveolae, was distributed in fractions 4–5, hereafter denoted as the caveolae fractions (Figure 3A). Mature and thus active forms of cathepsin B were also present in the caveolae fractions: 31 kDa single chain cathepsin B and 25/26 kDa heavy chain of double chain cathepsin B. The majority of cathepsin B was isolated in dense fractions 8–11, which contain lysosomes as identified using the lysosomal marker proteins LAMP-1 and β-galactosidase [34] (data not shown). To confirm that cathepsin B in the caveolae fractions was active, prior to subcellular fractionation, we pretreated HUVEC with a FITC-labeled activity-based probe (GB111-FL) that selectively and covalently binds the active sites of two cysteine cathepsins, cathepsin B and cathepsin L [25]. SDS-PAGE analysis and laser scanning imaging of subcellular fractions revealed only active cathepsin B (31 kDa) in the caveolae fractions (fractions 4 and 5) of HUVEC (Figure 3B). Active cathepsin B [25] and active cathepsin L (28 kDa) were present in the dense or lysosomal fractions (fractions 9 and 10). The presence of active cathepsin B in caveolae of HUVEC would be consistent with a functional significance for cathepsin B in these membrane microdomains as has been shown in human colon carcinoma

NIH-PA Author Manuscript

NIH-PA Author Manuscript

NIH-PA Author Manuscript

cells [34]. We have previously identified the light chain of AIIt, p11, as a cell surface binding partner for procathepsin B in human breast carcinoma and glioma cells [37] and determined that cathepsin B and p11 cosediment in caveolae fractions of HCT116 human colon carcinoma cells [34]. Here, we found p11 along with annexin II, the heavy chain of AIIt, localized to the caveolae of HUVEC (Figure 3A). This suggests that the association of cathepsin B with caveolae may be mediated by its binding partner p11.

Distribution of cathepsin B to caveolae of HUVEC increases during endothelial cell tube formation

We further examined the translocation of cathepsin B to caveolae in HUVEC cells during endothelial cell tube formation. Due to the large volume of rBM required to generate sufficient HUVEC tube-like structures for isolation of caveolae, we were not able to use sodium carbonate extraction and subcellular fractionation on a sucrose gradient to isolate caveolae. Therefore, we used an alternative approach of successive detergent extractions [30] that is based on the insolubility of caveolae in 1% Triton X-100. Cells grown as 2D monolayers and 3D tube-like structures were fractionated into Triton-soluble (TS) and Triton-insoluble (TI) fractions; lipid rich microdomains including caveolae are localized to TI fractions whereas proteins resident to other cellular organelles including lysosomes are found in the TS fraction [30]. The advantage of this method of caveolae isolation over the carbonate extraction method described above is that it preserves the stability and thus activity of proteases allowing us to measure enzymatic activity following fractionation. Cav-1 served as a positive control for the presence of caveolae in the TI-fraction (Figure 3C): however, it was also present in the TS-fraction since it is not exclusive to caveolae, but is found in the ER and Golgi prior to its association with lipids and formation of caveolae at the cell surface [38]. To confirm that caveolae were present in the TI-fraction, we treated HUVEC for one hour prior to successive detergent extraction with 10 mM MβCD, a cholesterol sequestering drug that disrupts the structure of caveolae. As a result, there was a loss in cav-1 distribution to the TI-fraction of treated cells (Figure 3D). Analysis of cathepsin B revealed an increase in the distribution of the mature 31 kDa and 25/26 kDa forms and the 38 kDa intermediate form to caveolae of HUVEC tube-like structures as compared to caveolae of monolayer HUVEC (Figure 3C); this association is lost following 10 mM MβCD treatment (Figure 3D), thus verifying that distribution of cathepsin B to caveolae is not an artifact of the fractionation procedure. Quantitation of the immunoblotting data in Figure 3C revealed a 15% increase in the distribution of cathepsin B to the TI fraction as compared to the TS fraction during HUVEC tube formation (data not shown). Similarly, the distribution of p11 to the TI fractions was increased during tube formation [90% increase (data not shown)] while the distribution of annexin II remained unchanged (Figure 3C). Enzymatic assays also detected increased cathepsin B activity in the caveolae fraction of HUVEC tube-like structures as compared to HUVEC monolayer, consistent with a functional role for this protease within these membrane domains (Figure 3E). Cathepsin B activity was also detected in the media conditioned during HUVEC tube formation at levels greater than that observed in the media conditioned by HUVEC grown as a monolayer on gelatin (Figure 3F). These data along with the pericellular degradation observed during tube formation suggest that association of cathepsin B with caveolae may increase cathepsin B secretion and ECM degradation during endothelial cell tube formation.

Collagen IV degradation products colocalize intracellularly with active cysteine cathepsins and cav-1

We performed live cell proteolysis assays with HUVEC transfected with cav-1-mRFP in the presence of GB-123, a non-quenched activity-based probe for cysteine cathepsins B and L [26]. Note that we used GB-123 (a Cy5 labeled probe) rather than GB111-FL in these live-cell proteolysis assays because the FITC-labeled GB111-FL cannot be differentiated from the degradation products of DQ-collagen IV. Cells grown in rBM containing DQ-collagen IV for

NIH-PA Author Manuscript

NIH-PA Author Manuscript

NIH-PA Author Manuscript

18 h in the presence of GB-123 were washed to remove unbound GB-123 and incubated 1–2 h in probe-free medium prior to imaging for DQ-collagen IV degradation, cav-1 and cysteine cathepsin activity (Figure 4). Our results revealed that DQ-collagen IV degradation products (green) partially colocalized intracellularly with cav-1-mRFP (red) and GB-123 (blue), thus providing further support for the functional significance of cathepsin B localizing to caveolae.

Redistribution of other ECM degrading proteases to HUVEC caveolae during tube formation

Cathepsin B has been previously described as a potential initiator of ECM proteolytic pathways that include proteases of the plasmin(ogen) cascade and MMPs. For that reason, we examined the distribution of pro-uPA, a cathepsin B substrate [10], and its receptor uPAR to caveolae of HUVEC during tube formation and found an increased association of both pro-uPA and uPAR to the TI fractions of HUVEC tube-like structures as compared to TI fractions of HUVEC monolayers (Figure 5A). β1-integrin, a protein that forms a trimeric complex with uPAR and cav-1 on cell surfaces, also co-colocalized to these caveolae fractions during tube formation (Figure 5A). These results are consistent with caveolae being the site for the initiation of a network of proteases involved in ECM degradation on the surface of endothelial cells.

MMP-2 and MMP-14 have both been identified in caveolae of glioblastomas, fibrosarcomas and endothelial cells [39,40]. We therefore examined the association of these MMPs with caveolae of HUVEC. MMP-14, also known as MT1-MMP, had previously been shown to localize to caveolae and to internalize and traffic through endothelial cells via a caveolae-mediated pathway [39–41]. In our studies, we detected an increased distribution of MMP-14 to caveolae (TI-fraction) of HUVEC during tube formation (Figure 5A).

We performed gelatin-zymography to compare the intracellular distribution of gelatinases MMP-2 and -9 in HUVEC grown as a monolayer versus tube-like structures. Our results revealed an association of MMP-2 with caveolae (TI) fractions of HUVEC following tube formation (Figure 5B). Although MMP-9 was detected in both the TS-and TI-fractions of HUVEC tube-like structures, we detected MMP-9 in the rBM (i.e., in the Cultrex used in the *in vitro* tube formation assays) in the absence of cells as well as in media conditioned by Cultrex in the absence of cells (data not shown). MMP-2, in contrast, was not detected in Cultrex in the absence of cells or in media conditioned by Cultrex in the absence of cells (data not shown).

Pericellular proteolysis of collagen IV by migrating HUVEC during tube formation

We performed live cell proteolysis assays in 4D (i.e., three-dimensional space + time) during endothelial tube formation. To conduct these assays, we seeded HUVEC onto rBM containing DQ-collagen IV and imaged the cells every 10 min over 16 h with a Zeiss LSM 510 META NLO microscope equipped with a controlled environmental chamber. Images taken at six time points over the course of the 16 h incubation period are illustrated in Figure 6A. A movie of proteolysis by the migrating and differentiating HUVEC is available online (Supplementary Materials, Movie SM1). After 2 h of incubation, HUVEC were still single cells with some cells exhibiting sprouting (arrowheads). By 4 h the cells had started to align and form small tubular networks with degradation products of DQ-collagen IV (green) present pericellularly. At 6 h and 12 h, the smaller networks had begun to coalesce into larger networks. By 14 h and 16 h, larger tubular structures had formed from the smaller tubes produced earlier during the assay (4 h) and degradation products were observed immediately adjacent to the tubes. We also observed pericellular degradation products of DQ-collagen IV at the rear of one cell (arrow) that was migrating towards the developing tubular structure. When we performed live cell proteolysis assays using HUVEC transfected with cav-1-mRFP, we found that DQ-collagen IV degradation products colocalized intracellularly with cav-1-mRFP in the perinuclear region. Degradation products were also found pericellularly at both the front and at the rear of a migrating endothelial cells (arrows) [Figure 6B and movie available online (Supplementary

NIH-PA Author Manuscript

NIH-PA Author Manuscript

NIH-PA Author Manuscript

Materials, Movie SM2)]. These data are quite intriguing since polarization of cav-1 to either the front or the rear of migrating cells including endothelial cells has been reported [20, 22, 42–44] and we detected cav-1 colocalized with DQ-collagen IV degradation products at the rear of migrating endothelial cells (see arrowhead in insert). These data are consistent with a role for caveolae-associated proteases in endothelial cell migration through ECM during tube formation.

Discussion

Differentiation of endothelial cells during angiogenesis is a process that involves proteolytic enzymes, which degrade basement membrane and thereby facilitate cell migration, invasion and capillary tube formation. The accessibility of proteases to the ECM is enhanced by their localization on the cell membrane. Here, we explored one possible mechanism for cell surface association, i.e., the distribution of cathepsin B and other proteases associated with ECM degradation to caveolae on the cell surface of endothelial cells. Our results are the first to show through live-cell imaging ECM degradation in association with active cathepsin B in caveolae of endothelial cells during tube formation.

Caveolae are abundant in endothelial cells [45] and during an angiogenic response caveolae appear to coalesce and form larger, vesicular structures [46]. Previous studies have shown a correlation between cav-1 expression and angiogenesis. Overexpression of cav-1 in endothelial cells enhances caveolae formation and accelerates capillary tube development [47] and, conversely, downregulation of cav-1 reduces the number of capillary tubes [23,47]. Moreover, caveolae are hypothesized to be sites for the compartmentalization of cell surface proteases [12], including proteases linked to angiogenesis. In the present study, we identified active cathepsin B and its cell surface receptor, p11, along with other ECM degrading proteases (i.e., pro-uPA, MMP-2 and -14), in caveolar fractions of human endothelial cells, an association that was enhanced during tube formation.

Cathepsin B regulates both pro- and anti-angiogenic factors suggesting that this enzyme may be a contributor to the “angiogenic switch” of endothelial cells [9]. Lack of cathepsin B reduces angiogenesis in a mouse model of pancreatic islet cell carcinogenesis (RIP1-Tag2) crossed with cathepsin B-null mice; in contrast, a lack of cathepsin L does not affect angiogenesis in this mouse model [48]. Cathepsin B also has been shown to exert anti-angiogenic affects through its ability to cleave collagen XVIII to generate endostatin, an anti-angiogenic factor that has been identified in caveolae of endothelial cells [11,49].

uPA also has variable roles in angiogenesis. Binding of uPA to its receptor, uPAR, enhances organization of endothelial cells into tubular structures [50]. Conversely, uPA, along with tissue plasminogen activator (tPA), mediates the generation of angiostatin, an anti-angiogenic factor, from plasminogen [51]. The increased levels of β1-integrin in caveolae of HUVEC may reflect intersections between proteolytic and signaling pathways observed in human chondrocytes in which uPAR complexes with cav-1 via β1-integrin [52] and disruption of this complex results in the loss of uPAR-dependent adhesion and β1-integrin-induced signal transduction [53]. Our findings of increased localization of p11, pro-uPA, uPAR and β1-integrin to caveolae of endothelial cells during tube formation would be consistent with a functional role for caveolae as a site for the compartmentalization and regulation of proteolytic events associated with angiogenesis.

Colocalization of cathepsin B and pro-uPA to caveolae of endothelial cells is interesting since cathepsin B can activate pro-uPA to uPA, thereby initiating a network of cell surface proteolytic events that includes activation of plasminogen and MMPs [10,54]. The associations of MMP-2 and -14 with endothelial caveolae, when the cells formed tubular structures, are in concert with

NIH-PA Author Manuscript

NIH-PA Author Manuscript

NIH-PA Author Manuscript

an increase in secretion of MMP-2. MMP-14 and MMP-2 have previously been localized to caveolae of endothelial cells along with αvβ3 and TIMP-2, a receptor and an inhibitor of MMP-2, respectively [39,40]. The colocalization of these proteins to caveolae may be of functional significance since MMP-14 activates MMP-2, a process that also involves TIMP-2 [55]. In endothelial cells, the cytoplasmic tail of MMP-14 binds phosphorylated cav-1 [56], and the enzyme is internalized and trafficked by caveolae-mediated endocytosis [41].

Although the mechanism(s) for translocation of proteases to caveolae remains unclear, we hypothesize that their localization to these specialized membrane domains influences their activities at the cell surface. Our previous studies in human colorectal carcinoma cells revealed that downregulation of cav-1 decreases distribution of cathepsin B and uPA to caveolae and secretion of these enzymes [18]. Consequentially, these cav-1 knockdown cells are less invasive and degrade less ECM than their parental counterparts [18]. In the present study, we show intracellular colocalization of cav-1 with ECM degradation products in endothelial cells. In particular, intracellular colocalization of ECM degradation products and cav-1 was observed at the rear of some endothelial cells migrating on rBM. Other studies have shown that cav-1 translocates to the rear of migrating endothelial cells [22]. Here we propose that a possible function for caveolae and their associated proteases at the rear of migrating endothelial cells is in the uptake and intracellular degradation of ECM proteins, a prerequisite for cell detachment and one that also has been observed for cathepsin B in migrating tumor cells [14]. An involvement of proteases in the intracellular degradation of ECM proteins has been reported [35,57–59]. In breast carcinoma cells, intracellular cysteine cathepsins degrade collagen IV [59], a process suppressed by CA074Me, a cell-permeable, selective inhibitor of cathepsins B and L [60]. Degradation of collagen IV by fibroblasts is also linked to cysteine cathepsins following endocytosis of collagen IV via a mechanism mediated by the uPAR-associated protein (uPARAP)/Endo180 [61], a member of the macrophage mannose receptor family of endocytic transmembrane glycoproteins [62]. uPARAP forms a trimeric complex with uPA and uPAR on the cell surface and binds several types of collagens including collagen I, IV and V [63]. In mice deficient in uPARAP, fibroblasts show an almost complete abrogation of collagen endocytosis and diminished cell adhesion and migration on various collagens [61]. Although there are no known reports on the expression of uPARAP in endothelial cells, its association with uPA/uPAR in other cell types leads us to speculate that uPARAP associates with caveolae and participates in ECM endocytosis and degradation. In Figure 7, we have illustrated a potential pathway for the association of proteases (i.e., cathepsin B, uPA and MMPs) with caveolae and caveolae-associated ECM degradation in endothelial cells. Further dissection of the mechanisms of ECM endocytosis and degradation via caveolae and their associated proteases in endothelial cell differentiation remains for future studies.

Acknowledgements

This work was supported by a National Institutes of Health (NIH) National Technology Center for Networks and Pathways Grant (U54-RR020843) and a DOD Breast Cancer Center of Excellence (DAMD17-02-1-0693). The Microscopy and Imaging Resources Laboratory is supported by the NIH National Technology Center Grant and NIH Center Grants P30-ES06639 and P30-CA22453.

References

1. Risau W. Mechanisms of angiogenesis. Nature 1997;386:671–674. [PubMed: 9109485]
2. van Hinsbergh VW, Engelse MA, Quax PH. Pericellular proteases in angiogenesis and vasculogenesis. Arterioscler Thromb Vasc Biol 2006;26:716–728. [PubMed: 16469948]
3. Bergers G, Brekken R, McMahon G, Vu TH, Itoh T, Tamaki K, Tanzawa K, Thorpe P, Itohara S, Werb Z, Hanahan D. Matrix metalloproteinase-9 triggers the angiogenic switch during carcinogenesis. Nat Cell Biol 2000;2:737–744. [PubMed: 11025665]

NIH-PA Author Manuscript

NIH-PA Author Manuscript

NIH-PA Author Manuscript

4. Pepper MS. Role of the matrix metalloproteinase and plasminogen activator-plasmin systems in angiogenesis. Arterioscler Thromb Vasc Biol 2001;21:1104–1117. [PubMed: 11451738]
5. Rakic JM, Maillard C, Jost M, Bajou K, Masson V, Devy L, Lambert V, Foidart JM, Noel A. Role of plasminogen activator-plasmin system in tumor angiogenesis. Cell Mol Life Sci 2003;60:463–473. [PubMed: 12737307]
6. Preissner KT, May AE, Wohn KD, Germer M, Kanse SM. Molecular crosstalk between adhesion receptors and proteolytic cascades in vascular remodelling. Thromb Haemost 1997;78:88–95. [PubMed: 9198134]
7. Xu J, Rodriguez D, Petitclerc E, Kim JJ, Hangai M, Moon YS, Davis GE, Brooks PC. Proteolytic exposure of a cryptic site within collagen type IV is required for angiogenesis and tumor growth in vivo. J Cell Biol 2001;154:1069–1079. [PubMed: 11535623]
8. Patterson BC, Sang QA. Angiostatin-converting enzyme activities of human matrilysin (MMP-7) and gelatinase B/type IV collagenase (MMP-9). J Biol Chem 1997;272:28823–28825. [PubMed: 9360944]
9. Im E, Venkatakrishnan A, Kazlauskas A. Cathepsin B regulates the intrinsic angiogenic threshold of endothelial cells. Mol Biol Cell 2005;16:3488–3500. [PubMed: 15901832]
10. Kobayashi H, Schmitt M, Goretzki L, Chucholowski N, Calvete J, Kramer M, Gunzler WA, Janicke F, Graeff H. Cathepsin B efficiently activates the soluble and the tumor cell receptor-bound form of the proenzyme urokinase-type plasminogen activator (Pro-uPA). J Biol Chem 1991;266:5147–5152. [PubMed: 1900515]
11. Ferreras M, Felbor U, Lenhard T, Olsen BR, Delaisse J. Generation and degradation of human endostatin proteins by various proteinases. FEBS Lett 2000;486:247–251. [PubMed: 11119712]
12. Cavallo-Medved D, Sloane BF. Cell-surface cathepsin B: understanding its functional significance. Curr Top Dev Biol 2003;54:313–341. [PubMed: 12696754]
13. Fridman R, Toth M, Chvyrkova I, Meroueh SO, Mobashery S. Cell surface association of matrix metalloproteinase-9 (gelatinase B). Cancer Metastasis Rev 2003;22:153–166. [PubMed: 12784994]
14. Mohamed MM, Sloane BF. Cysteine cathepsins: multifunctional enzymes in cancer. Nat Rev Cancer 2006;6:764–775. [PubMed: 16990854]
15. Seiki M, Koshikawa N, Yana I. Role of pericellular proteolysis by membrane-type 1 matrix metalloproteinase in cancer invasion and angiogenesis. Cancer Metastasis Rev 2003;22:129–143. [PubMed: 12784992]
16. Anderson RG. The caveolae membrane system. Annu Rev Biochem 1998;67:199–225. [PubMed: 9759488]
17. Williams TM, Lisanti MP. The caveolin proteins. Genome Biol 2004;5:214. [PubMed: 15003112]
18. Cavallo-Medved D, Mai J, Dosescu J, Sameni M, Sloane BF. Caveolin-1 mediates the expression and localization of cathepsin B, pro-urokinase plasminogen activator and their cell-surface receptors in human colorectal carcinoma cells. J Cell Sci 2005;118:1493–1503. [PubMed: 15769846]
19. Massimino ML, Griffoni C, Spisni E, Toni M, Tomasi V. Involvement of caveolae and caveolae-like domains in signalling, cell survival and angiogenesis. Cell Signal 2002;14:93–98. [PubMed: 11781132]
20. Beardsley A, Fang K, Mertz H, Castranova V, Friend S, Liu J. Loss of caveolin-1 polarity impedes endothelial cell polarization and directional movement. J Biol Chem 2005;280:3541–3547. [PubMed: 15504729]
21. Isshiki M, Ando J, Yamamoto K, Fujita T, Ying Y, Anderson RG. Sites of Ca(2+) wave initiation move with caveolae to the trailing edge of migrating cells. J Cell Sci 2002;115:475–484. [PubMed: 11861755]
22. Parat MO, Anand-Apte B, Fox PL. Differential caveolin-1 polarization in endothelial cells during migration in two and three dimensions. Mol Biol Cell 2003;14:3156–3168. [PubMed: 12925753]
23. Griffoni C, Spisni E, Santi S, Riccio M, Guarnieri T, Tomasi V. Knockdown of caveolin-1 by antisense oligonucleotides impairs angiogenesis in vitro and in vivo. Biochem Biophys Res Commun 2000;276:756–761. [PubMed: 11027543]
24. Moin K, Day NA, Sameni M, Hasnain S, Hirama T, Sloane BF. Human tumour cathepsin B. Comparison with normal liver cathepsin B. Biochem J 1992;285:427–434. [PubMed: 1637335]

NIH-PA Author Manuscript

NIH-PA Author Manuscript

NIH-PA Author Manuscript

25. Blum G, Mullins SR, Keren K, Fonovic M, Jedeszko C, Rice MJ, Sloane BF, Bogyo M. Dynamic imaging of protease activity with fluorescently quenched activity-based probes. Nature Chem Biol 2005;1:203–209. [PubMed: 16408036]
26. Blum G, von Degenfeld G, Merchant MJ, Blau HM, Bogyo M. Noninvasive optical imaging of cysteine protease activity using fluorescently quenched activity-based probes. Nature Chem Biol 2007;3:668–677. [PubMed: 17828252]
27. Grant DS, Lelkes PI, Fukuda K, Kleinman HK. Intracellular mechanisms involved in basement membrane induced blood vessel differentiation in vitro. In Vitro Cell Dev Biol 1991;27A:327–336. [PubMed: 1856158]
28. Kubota Y, Kleinman HK, Martin GR, Lawley TJ. Role of laminin and basement membrane in the morphological differentiation of human endothelial cells into capillary-like structures. J Cell Biol 1988;107:1589–1598. [PubMed: 3049626]
29. Song KS, Li S, Okamoto T, Quilliam LA, Sargiacomo M, Lisanti MP. Co-purification and direct interaction of Ras with caveolin, an integral membrane protein of caveolae microdomains. Detergent-free purification of caveolae microdomains. J Biol Chem 1996;271:9690–9697. [PubMed: 8621645]
30. Solomon KR, Mallory MA, Finberg RW. Determination of the non-ionic detergent insolubility and phosphoprotein associations of glycosylphosphatidylinositol-anchored proteins expressed on T cells. Biochem J 1998;334:325–333. [PubMed: 9716490]
31. Toth M, Gervasi DC, Fridman R. Phorbol Ester-induced Cell Surface Association of Matrix Metalloproteinase-9 in Human MCF1OA Breast Epithelial Cells. Cancer Res 1997;57:3159–3167. [PubMed: 9242444]
32. Linebaugh BE, Sameni M, Day NA, Sloane BF, Keppler D. Exocytosis of active cathepsin B enzyme activity at pH 7.0, inhibition and molecular mass. Eur J Biochem 1999;264:100–109. [PubMed: 10447678]
33. Caglic D, Pungercar JR, Pejler G, Turk V, Turk B. Glycosaminoglycans facilitate procathepsin B activation through disruption of propeptide-mature enzyme interactions. J Biol Chem 2007;282:33076–33085. [PubMed: 17726009]
34. Cavallo-Medved D, Dosescu J, Linebaugh B, Sameni M, Rudy D, Sloane BF. Mutant K-ras regulates cathepsin B localization on the surface of human colorectal carcinoma cells. Neoplasia 2003;5:507–519. [PubMed: 14965444]
35. Sameni M, Dosescu J, Moin K, Sloane BF. Functional imaging of proteolysis: stromal and inflammatory cells increase tumor proteolysis. Mol Imaging 2003;2:159–175. [PubMed: 14649059]
36. Sloane BF, Sameni M, Podgorski I, Cavallo-Medved D, Moin K. Functional imaging of tumor proteolysis. Annu Rev Pharmcol Toxicol 2006;46:301–315.
37. Mai J, Waisman DM, Sloane BF. Cell surface complex of cathepsin B/annexin II tetramer in malignant progression. Biochim Biophys Acta 2000;1477:215–230. [PubMed: 10708859]
38. Liu P, Rudick M, Anderson RG. Multiple functions of caveolin-1. J Biol Chem 2002;277:41295–41298. [PubMed: 12189159]
39. Annabi B, Lachambre M, Bousquet-Gagnon N, Page M, Gingras D, Beliveau R. Localization of membrane-type 1 matrix metalloproteinase in caveolae membrane domains. Biochem J 2001;353:547–553. [PubMed: 11171051]
40. Puyraimond A, Fridman R, Lemesle M, Arbeille B, Menashi S. MMP-2 colocalizes with caveolae on the surface of endothelial cells. Exp Cell Res 2001;262:28–36. [PubMed: 11120602]
41. Galvez BG, Matias-Roman S, Yanez-Mo M, Vicente-Manzanares M, Sanchez-Madrid F, Arroyo AG. Caveolae are a novel pathway for membrane-type 1 matrix metalloproteinase traffic in human endothelial cells. Mol Biol Cell 2004;15:678–687. [PubMed: 14657245]
42. Santilman V, Baran J, Anand-Apte B, Fox PL, Parat MO. Caveolin-1 polarization in migrating endothelial cells is directed by substrate topology not chemoattractant gradient. Cell Motil Cytoskeleton 2006;63:673–680. [PubMed: 16960885]
43. Lentini D, Guzzi F, Pimpinelli F, Zaninetti R, Cassetti A, Coco S, Maggi R, Parenti M. Polarization of caveolins and caveolae during migration of immortalized neurons. J Neurochem 2008;104:514–523. [PubMed: 17986234]

NIH-PA Author Manuscript

NIH-PA Author Manuscript

NIH-PA Author Manuscript

44. Sun XH, Flynn DC, Castranova V, Millecchia LL, Beardsley AR, Liu J. Identification of a novel domain at the N terminus of caveolin-1 that controls rear polarization of the protein and caveolae formation. J Biol Chem 2007;282:7232–7241. [PubMed: 17213184]
45. Lisanti MP, Scherer PE, Vidugiriene J, Tang Z, Hermanowski-Vosatka A, Tu YH, Cook RF, Sargiacomo M. Characterization of caveolin-rich membrane domains isolated from an endothelial-rich source: implications for human disease. J Cell Biol 1994;126:111–126. [PubMed: 7517942]
46. Esser S, Wolburg K, Wolburg H, Breier G, Kurzchalia T, Risau W. Vascular endothelial growth factor induces endothelial fenestrations in vitro. J Cell Biol 1998;140:947–959. [PubMed: 9472045]
47. Liu J, Wang XB, Park DS, Lisanti MP. Caveolin-1 expression enhances endothelial capillary tubule formation. J Biol Chem 2002;277:10661–10668. [PubMed: 11748236]
48. Gocheva V, Zeng W, Ke D, Klimstra D, Reinheckel T, Peters C, Hanahan D, Joyce JA. Distinct roles for cysteine cathepsin genes in multistage tumorigenesis. Genes Dev 2006;20:543–556. [PubMed: 16481467]
49. Wickstrom SA, Alitalo K, Keski-Oja J. Endostatin associates with lipid rafts and induces reorganization of the actin cytoskeleton via down-regulation of RhoA activity. J Biol Chem 2003;278:37895–37901. [PubMed: 12851410]
50. Schnaper HW, Barnathan ES, Mazar A, Maheshwari S, Ellis S, Cortez SL, Baricos WH, Kleinman HK. Plasminogen activators augment endothelial cell organization in vitro by two distinct pathways. J Cell Physiol 1995;165:107–118. [PubMed: 7559792]
51. Gately S, Twardowski P, Stack MS, Cundiff DL, Grella D, Castellino FJ, Enghild J, Kwaan HC, Lee F, Kramer RA, Volpert O, Bouck N, Soff GA. The mechanism of cancer-mediated conversion of plasminogen to the angiogenesis inhibitor angiostatin. Proc Natl Acad Sci USA 1997;94:10868–10872. [PubMed: 9380726]
52. Schwab W, Gavlik JM, Beichler T, Funk RH, Albrecht S, Magdolen V, Luther T, Kasper M, Shakibaei M. Expression of the urokinase-type plasminogen activator receptor in human articular chondrocytes: association with caveolin and beta 1-integrin. Histochem Cell Biol 2001;115:317–323. [PubMed: 11405060]
53. Wei Y, Yang X, Liu Q, Wilkins JA, Chapman HA. A role for caveolin and the urokinase receptor in integrin-mediated adhesion and signaling. J Cell Biol 1999;144:1285–1294. [PubMed: 10087270]
54. Ikeda Y, Ikata T, Mishiro T, Nakano S, Ikebe M, Yasuoka S. Cathepsins B and L in synovial fluids from patients with rheumatoid arthritis and the effect of cathepsin B on the activation of pro-urokinase. J Med Invest 2000;47:61–75. [PubMed: 10740981]
55. Bernardo MM, Fridman R. TIMP-2 (tissue inhibitor of metalloproteinase-2) regulates MMP-2 (matrix metalloproteinase-2) activity in the extracellular environment after pro-MMP-2 activation by MT1 (membrane type 1)-MMP. Biochem J 2003;374:739–745. [PubMed: 12755684]
56. Labrecque L, Nyalendo C, Langlois S, Durocher Y, Roghi C, Murphy G, Gingras D, Beliveau R. Src-mediated tyrosine phosphorylation of caveolin-1 induces its association with membrane type 1 matrix metalloproteinase. J Biol Chem 2004;279:52132–52140. [PubMed: 15466865]
57. Everts V, van der Zee E, Creemers L, Beertsen W. Phagocytosis and intracellular digestion of collagen, its role in turnover and remodelling. Histochem J 1996;28:229–245. [PubMed: 8762055]
58. Kjoller L, Engelholm LH, Hoyer-Hansen M, Dano K, Bugge TH, Behrendt N. uPARAP/endo180 directs lysosomal delivery and degradation of collagen IV. Exp Cell Res 2004;293:106–116. [PubMed: 14729061]
59. Sameni M, Moin K, Sloane BF. Imaging proteolysis by living human breast cancer cells. Neoplasia 2000;2:496–504. [PubMed: 11228542]
60. Buttle DJ, Murata M, Knight CG, Barrett AJ. CA074 methyl ester: a proinhibitor for intracellular cathepsin B. Arch Biochem Biophys 1992;299:377–380. [PubMed: 1444478]
61. Engelholm LH, List K, Netzel-Arnett S, Cukierman E, Mitola DJ, Aaronson H, Kjoller L, Larsen JK, Yamada KM, Strickland DK, Holmbeck K, Dano K, Birkedal-Hansen H, Behrendt N, Bugge TH. uPARAP/Endo180 is essential for cellular uptake of collagen and promotes fibroblast collagen adhesion. J Cell Biol 2003;160:1009–1015. [PubMed: 12668656]
62. East L, Isacke CM. The mannose receptor family. Biochim Biophys Acta 2002;1572:364–386. [PubMed: 12223280]

NIH-PA Author Manuscript

NIH-PA Author Manuscript

NIH-PA Author Manuscript

63. Behrendt N. The urokinase receptor (uPAR) and the uPAR-associated protein (uPARAP/Endo180): membrane proteins engaged in matrix turnover during tissue remodeling. Biol Chem 2004;385:103–136. [PubMed: 15101555]

NIH-PA Author Manuscript
NIH-PA Author Manuscript
NIH-PA Author Manuscript

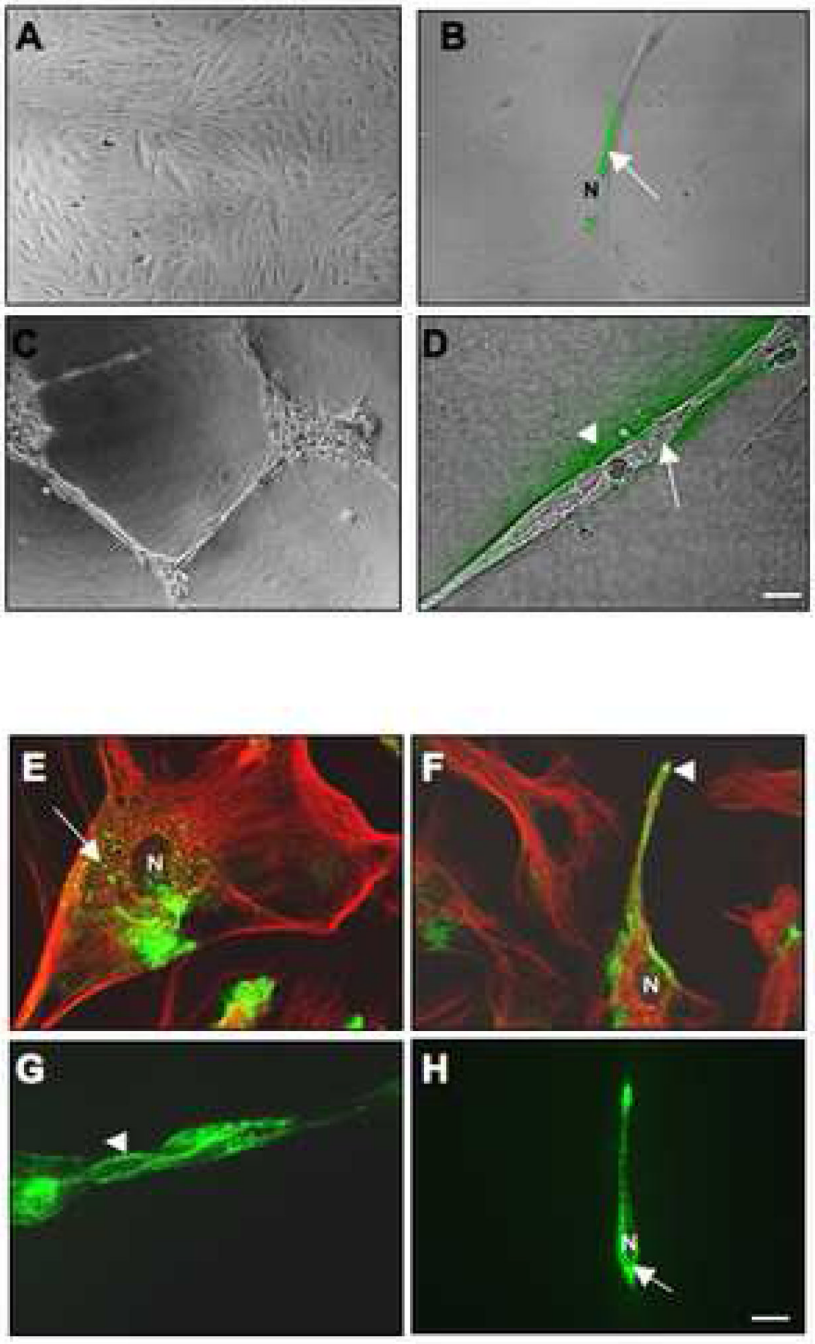

Figure 1. Gelatin and collagen IV degradation by and localization of endogenous cav-1 in HUVEC grown as a monolayer versus tube-like structures

Equal numbers of HUVEC were grown for 16 h on glass coverslips coated with gelatin alone (**A**), gelatin containing 25 μg/ml DQ-gelatin (**B**), rBM (Cultrex) alone (**C**), or rBM containing 25 μg/ml DQ-collagen IV (**D**). After 16 h, confocal images were taken of live cells [differential interference contrast (DIC)] and DQ-substrate degradation products (green), which are present intracellularly (arrow) in HUVEC grown on gelatin (**B**) and both intracellularly (arrow) and pericellularly (arrowhead) in HUVEC grown on rBM (**D**). Immunostaining for endogenous cav-1 using rabbit anti-human caveolin antibodies was performed on fixed and permeabilized HUVEC cells grown on gelatin (**E and F;** two different fields of view) or rBM (**G and H;** two

different fields of view). The morphology of HUVEC in monolayer culture is apparent from the immunostaining for tubulin (red) using mouse anti-human tubulin antibodies (**E and F**). Staining for caveolin is observed in the perinuclear region (arrow) and at the cell surface (arrowhead). N, nucleus. Bar, 20 μm.

NIH-PA Author Manuscript
NIH-PA Author Manuscript
NIH-PA Author Manuscript

NIH-PA Author Manuscript

NIH-PA Author Manuscript

NIH-PA Author Manuscript

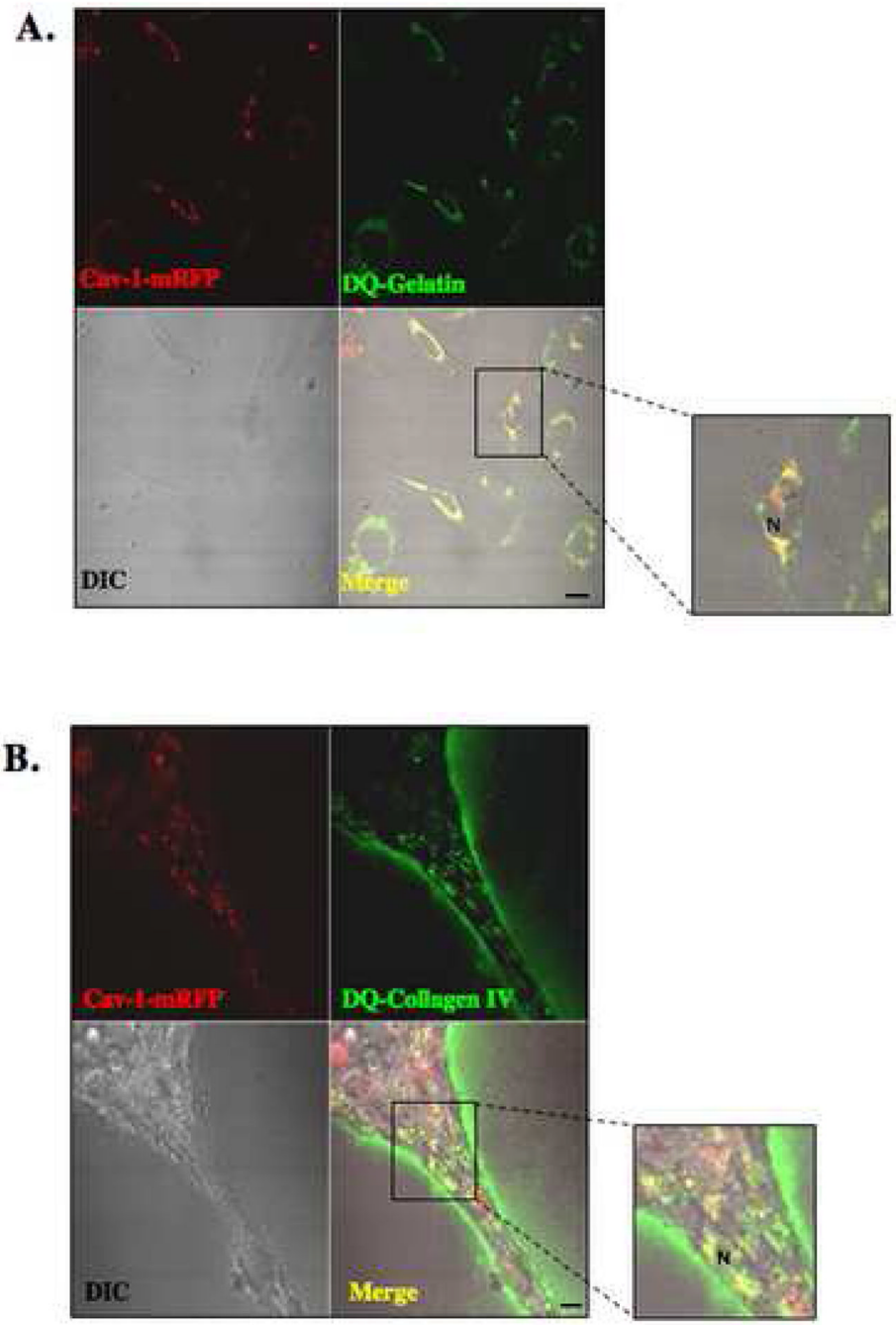

Figure 2. Intracellular colocalization of cav-1 with gelatin and collagen IV degradation products in HUVEC

Equal numbers of HUVEC transfected with cav-1-mRFP construct were grown for 16 h on glass coverslips coated with either gelatin containing 25 μg/ml DQ-gelatin (**A**) or rBM (Cultrex) containing 25 μg/ml DQ-collagen IV (**B**). After 16 h, confocal images were taken of live cells (DIC), cav-1-mRFP (red) and DQ-substrate degradation products (green). DQ-substrate degradation products (green) are present intracellularly in HUVEC grown on gelatin and both intracellularly and pericellularly in HUVEC grown on rBM (see inserts). Colocalization of cav-1-mRFP and DQ-substrate degradation products appears yellow in the merged images. N, nucleus. Bar, 20 μm.

NIH-PA Author Manuscript

NIH-PA Author Manuscript

NIH-PA Author Manuscript

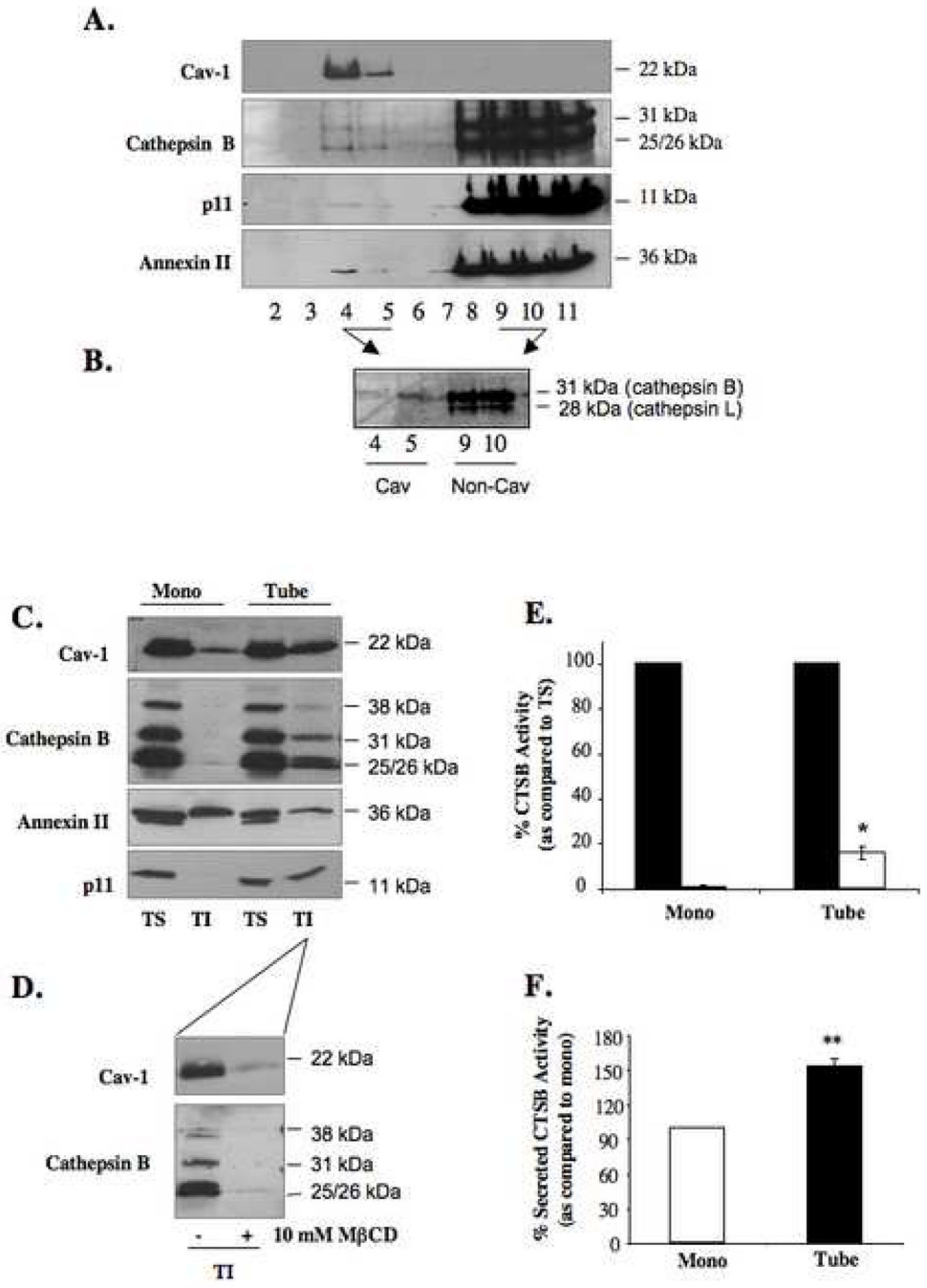

Figure 3. Increased distribution of active cathepsin B and p11 to caveolae of HUVEC cells during tube formation

HUVEC grown as a monolayer were subjected to subcellular fractionation on a sucrose gradient following homogenization in sodium carbonate buffer, pH 11.0. One ml fractions were collected from the top of the gradient and equal volume aliquots of fractions 2–11 were analyzed by SDS-PAGE and immunoblotted with anti-caveolin, anti-cathepsin B, anti-annexin II and anti-p11 antibodies (**A**). Aliquots from caveolae fractions 4 and 5 (Cav) and non-caveolae fractions 9 and 10 (non-Cav) isolated from HUVEC treated with 1μM GB111-FL were analyzed by SDS-PAGE and imaged using a Typhoon laser scanner. Cathepsin B (31 kDa) and cathepsin L (28 kDa) were labeled (**B**). Equal numbers of HUVEC were grown on gelatin

NIH-PA Author Manuscript

NIH-PA Author Manuscript

NIH-PA Author Manuscript

(mono) or rBM (tube) for 18 h and caveolae were isolated by successive detergent extraction as described in Materials and Methods. Triton-soluble (TS) represents non-caveolae fractions and Triton-insoluble (TI) represents caveolae fractions. Equal volume aliquots of each fraction were analyzed by SDS-PAGE and immunoblotted with anti-caveolin, anti-cathepsin B, anti-annexin II and anti-p11 antibodies (**C**). To verify distribution of caveolae to TI fractions, HUVEC grown for 18 h on rBM were treated with 10 mM MβCD for 1 h at 37 °C prior to caveolae isolation (**D**). TS (closed bars) and TI (open bars) fractions of HUVEC monolayers (mono) and tube-like structures (tube) were assayed for cathepsin B (CTSB) activity against Z-Arg-Arg-NHMec substrate and activity was recorded as pmol/min/cell number. The specific activity for caveolae-associated cathepsin B activity is expressed as a percentage of cathepsin B activity in the non-caveolar fraction (TS) (**E**). Overnight conditioned media of HUVEC grown as a monolayer on gelatin (mono) and during tube formation (tube) were also analyzed for cathepsin B activity and expressed as a percentage of secreted activatable cathepsin B activity from monolayer HUVEC (**F**). Immunoblots and graphs, presented as mean ± standard deviation, are representative of at least three experiments. * $P < 0.05$ and ** $P < 0.01$.

NIH-PA Author Manuscript
NIH-PA Author Manuscript
NIH-PA Author Manuscript

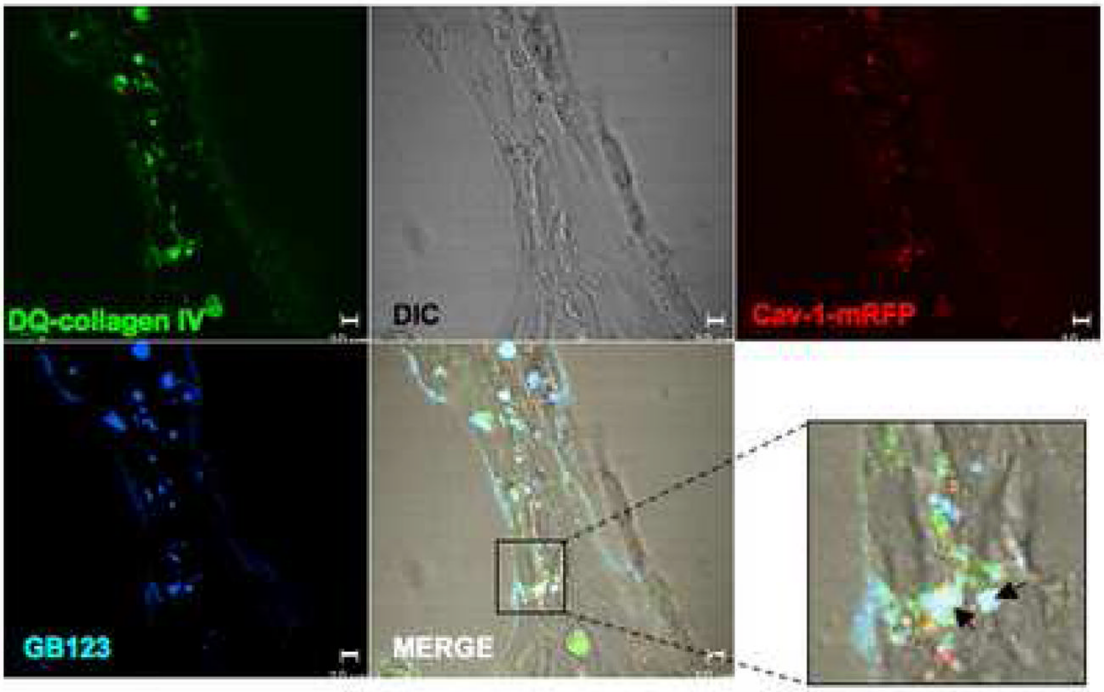

Figure 4. Active cathepsin B partially localizes to caveolae of HUVEC during tube formation

HUVEC were transiently transfected with a cav-1-mRFP construct and grown on glass coverslips coated with rBM containing 25 μg/ml DQ-collagen IV in the presence of 1 μM GB-123 for 18 h. Thereafter, unbound GB-123 was washed away and cells incubated 1–2 h in probe-free medium. Confocal images were then taken of live cells (DIC), cav-1-mRFP (red), DQ-collagen IV degradation products (green) and GB-123 bound to cysteine cathepsins (pseudocolored blue). Colocalization of cav-1-mRFP and DQ-collagen IV degradation products appears yellow, colocalization of DQ-collagen IV degradation products and GB-123 appears pale blue, and colocalization of cav-1-mRFP, DQ-collagen IV degradation products and GB-123 appears white (arrows; see insert) in the merged image. Bar, 10 μm.

NIH-PA Author Manuscript

NIH-PA Author Manuscript

NIH-PA Author Manuscript

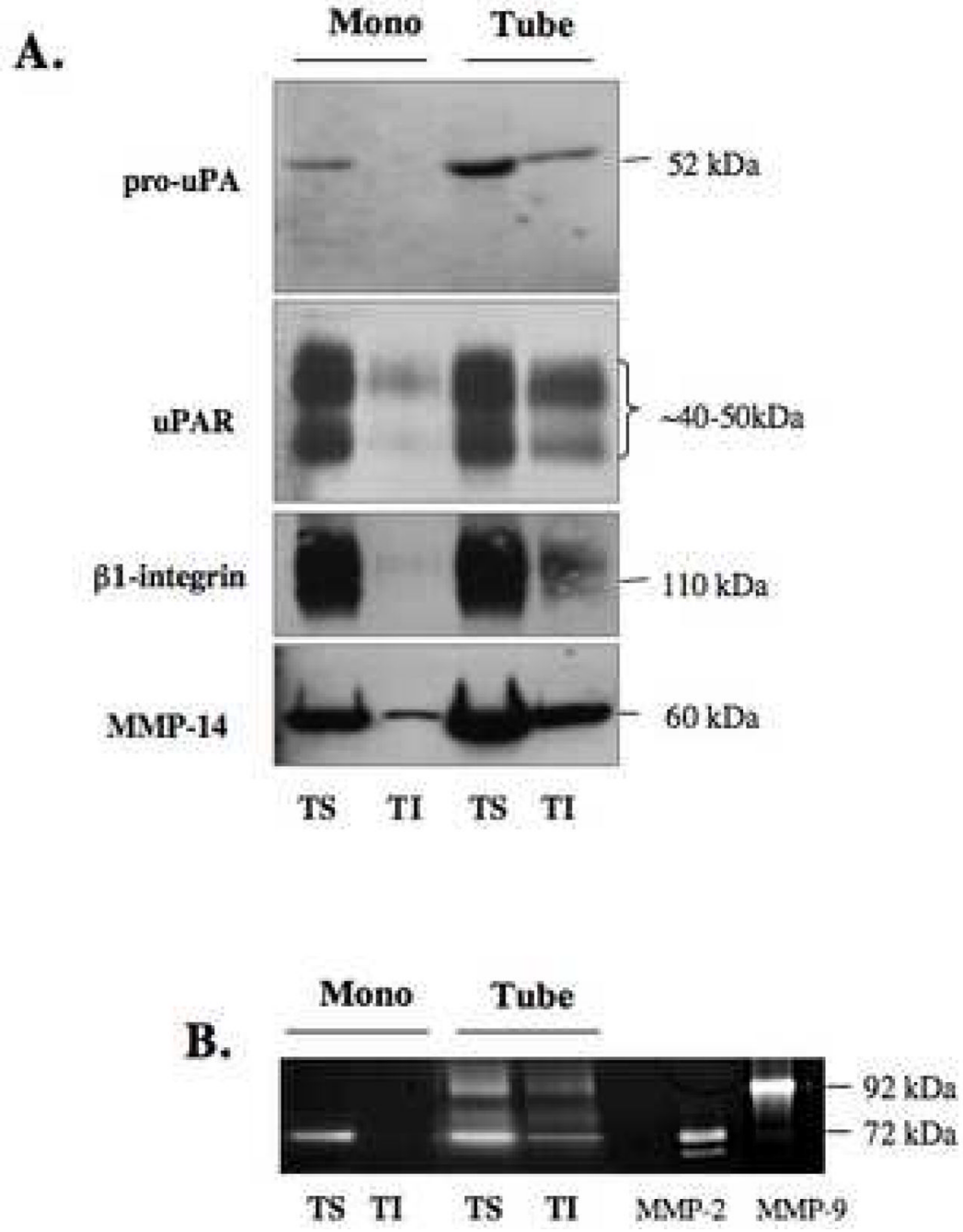

Figure 5. Increased distribution of pro-uPA, uPAR, β1-integrin, MMP-2 and MMP-14 to HUVEC caveolae during tube formation

Equal numbers of HUVEC were grown on gelatin (mono) or rBM (tubes) for 18 h and caveolae were isolated by successive detergent extraction as described in Materials and Methods. Triton-soluble (TS) represents non-caveolae fractions and Triton-insoluble (TI) represents caveolae fractions. Equal volume aliquots of each fraction were analyzed by SDS-PAGE and immunoblotted with anti-uPA, anti-uPAR, anti-β1-integrin and anti-MMP-14 antibodies (**A**). Equal volume aliquots of each fraction were also analyzed by gelatin zymography for MMP-2 and MMP-9 activities (**D**). Purified MMP-2 (10 ng) and MMP-9 (5 ng) were used as positive controls. Immunoblots and zymograms are representative of at least three experiments.

NIH-PA Author Manuscript
NIH-PA Author Manuscript
NIH-PA Author Manuscript

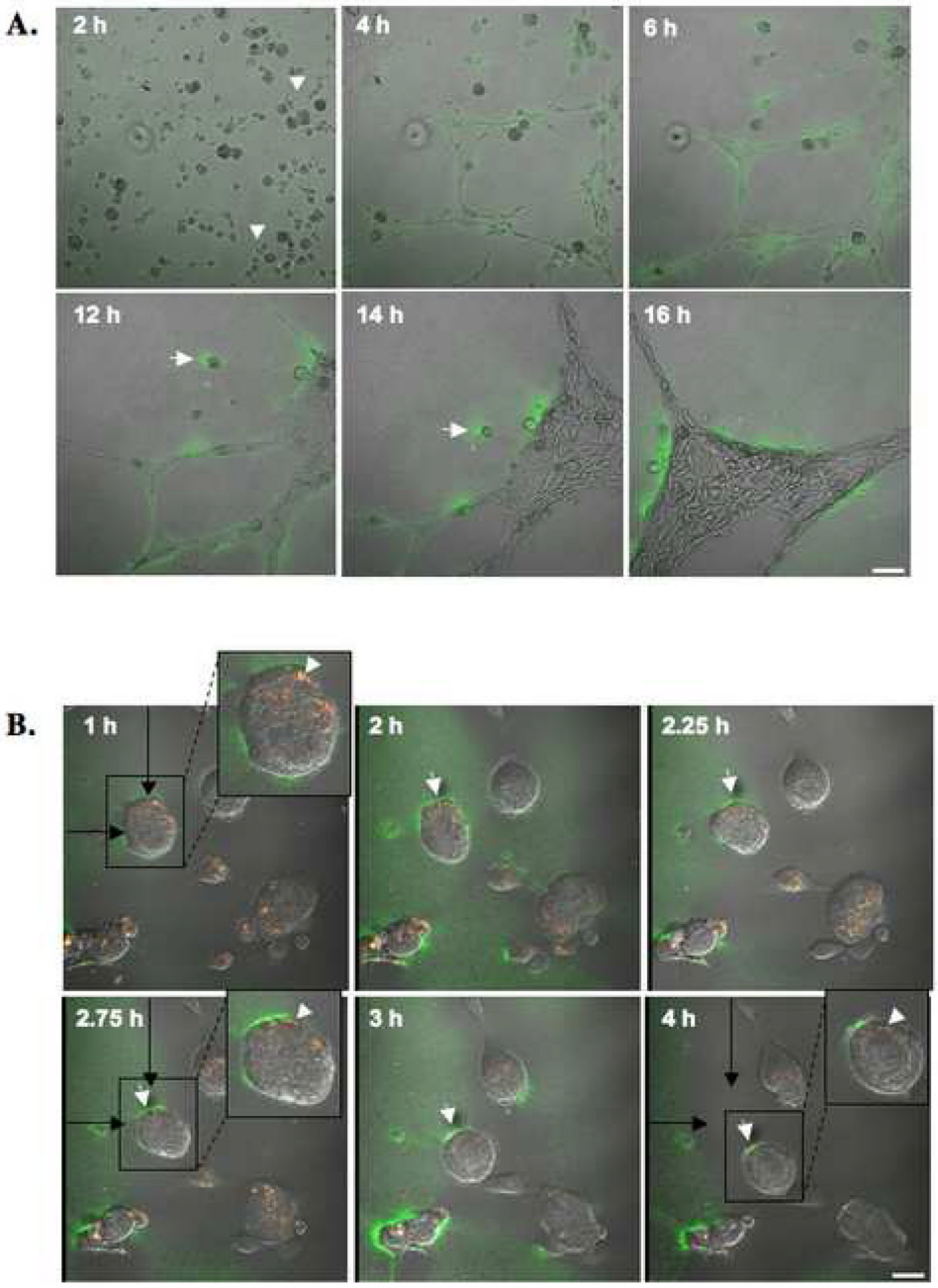

Figure 6. Time courses for collagen IV proteolysis and colocalization of collagen IV degradation products with cav-1 during HUVEC tube formation

HUVEC were grown on glass coverslips coated with rBM containing 25 μg/ml DQ-collagen IV. (**A**) Confocal images were taken of live cells between 2 and 16 h. DQ-collagen IV degradation products (green) are seen surrounding tubular structures and at the rear of a migrating endothelial cell (arrow). Cell sprouting is observed at 2h (arrowheads). Bar, 100 μm. (**B**) Confocal images were taken between 1 and 4 h of live HUVEC transfected with cav-1-mRFP. DQ-collagen IV degradation products (green) and cav-1 (red) are seen colocalized (yellow) intracellularly (arrowheads) and pericellular degradation of DQ-collagen IV is observed at the rear of a migrating endothelial cell (arrows). Black arrows represent the original location of a migrating HUVEC cell (in box) at 1h. Bar, 20 μm.

NIH-PA Author Manuscript

NIH-PA Author Manuscript

NIH-PA Author Manuscript

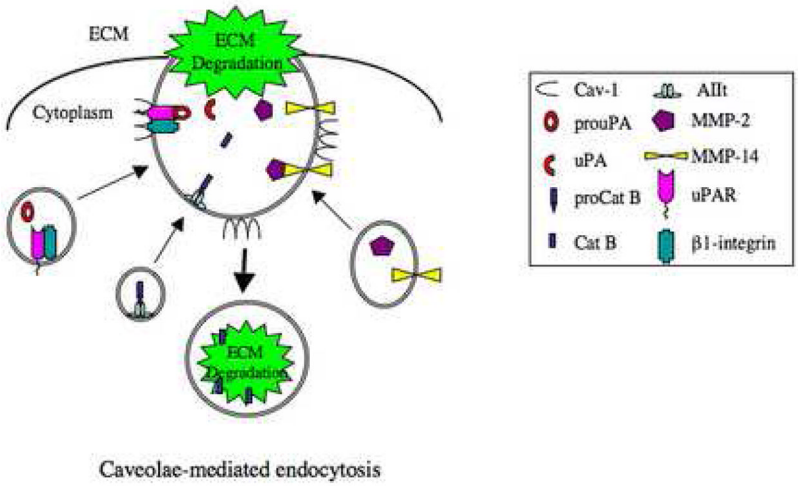

Figure 7. Potential protease network in endothelial cell caveolae during ECM degradation

In endothelial cells, proteases (i.e., cathepsin B, pro-uPA and MMPs) and their associated proteins/receptors (i.e., AIIt, uPAR and β1-integrin) are translocated to cell surface caveolae via intracellular vesicles (i.e., multivesicular bodies and exosomes) [14]. Caveolae-associated proteases are activated and degrade ECM proteins both pericellularly and intracellularly via caveolae-mediated endocytosis.